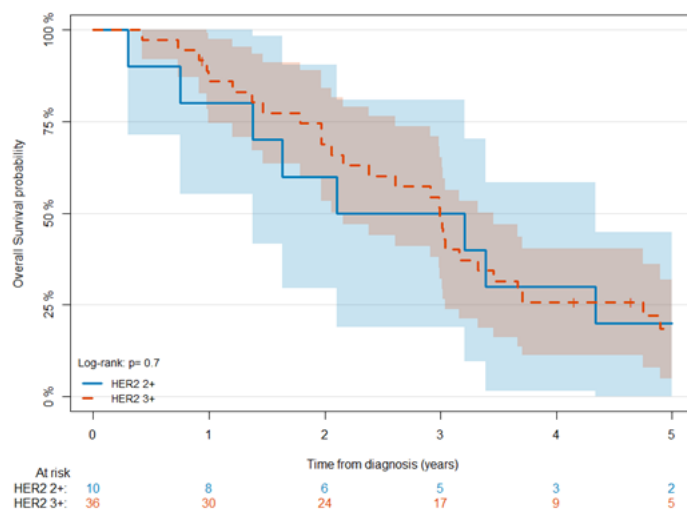


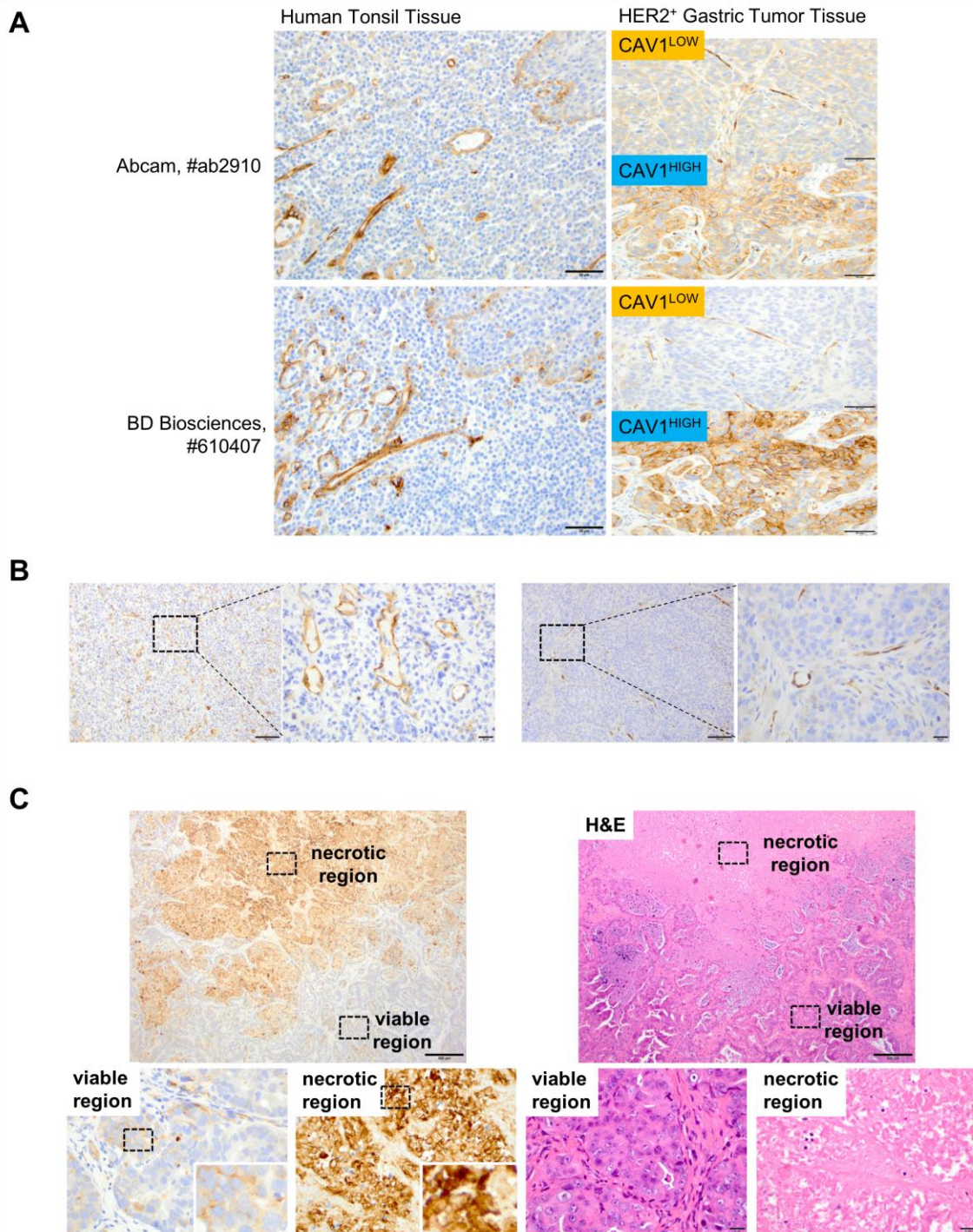
Pereira P. *et al*, Caveolin-1 temporal modulation enhances antibody drug efficacy in heterogeneous gastric cancer

SUPPLEMENTARY INFORMATION

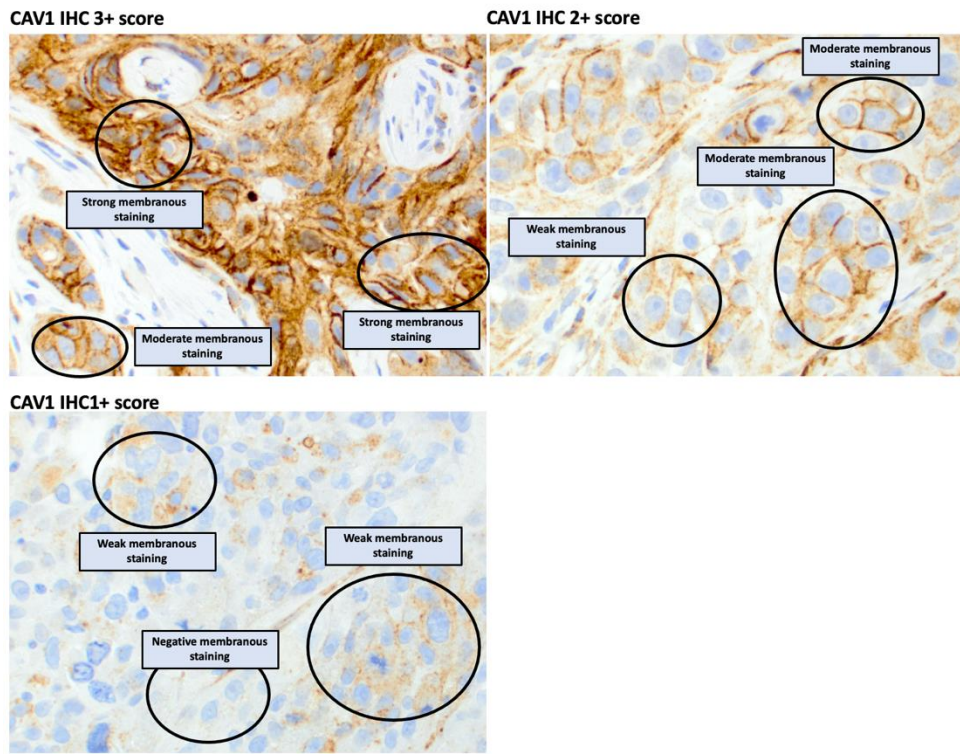


Characteristic	At 2 years	At 5 years
Group		
HER2 2+	60% (30%, 90%)	20% (0%, 45%)
HER2 3+	69% (53%, 84%)	18% (4.9%, 32%)

Supplementary Figure 1. Kaplan-Meier analyses of HER2 IHC 2+ versus 3+ and GC disease outcome in patients with gastric cancer treated with Trastuzumab ($n = 46$ patients).



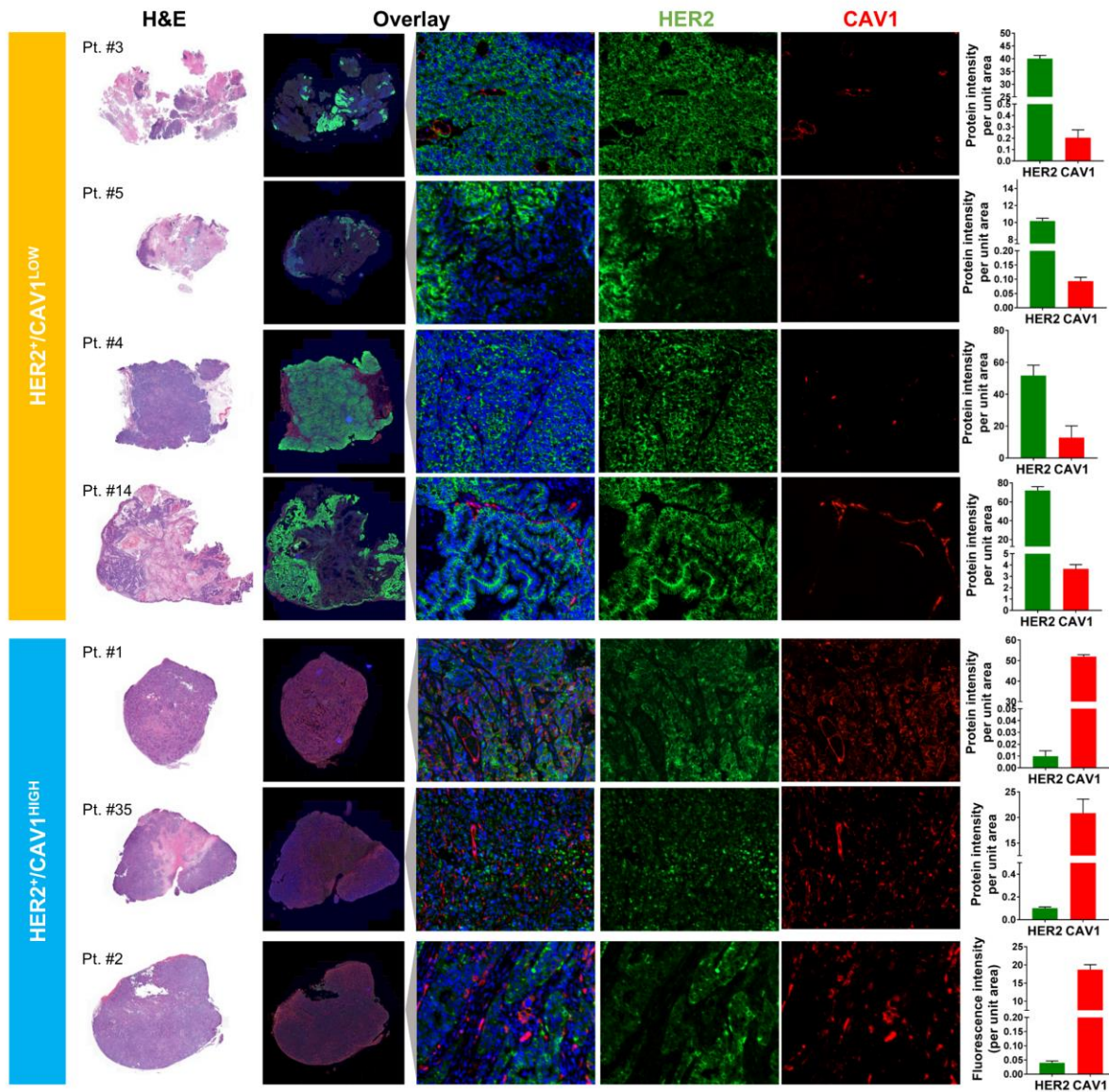
Supplementary Figure 2. (A) Immunohistochemical detection of CAV1 in human tonsil tissues (left panel) and HER2-expressing gastric tumor tissues using anti-CAV1 antibodies from Abcam (ab2910) or BD Biosciences (610407). CAV1 reactivity is present mainly in the blood vessels of human tonsils with weak epithelial reactivity. In gastric tumor tissues, CAV1 is present in both tumor and vascular endothelium. The anti-CAV1 antibody from BD Biosciences was used in future staining of HER2-expressing gastric tumor tissues as this was the one with the lowest unspecific binding. Scale bar, 50 μ m. (B) Representative images (scale bar, 100 μ m) with magnification (scale bar, 20 μ m) of CAV1 staining in the vascular endothelium but not in tumor cells. CAV1 IHC scoring analyses excluded staining in the vascular endothelium. (C) Representative images of CAV1 IHC 1+ membrane associated staining of tumor cells in viable regions versus strong nonspecific staining of necrotic tumor areas. CAV1 staining in necrotic regions was excluded during the IHC scoring analyses. Scale bar, 200 μ m.



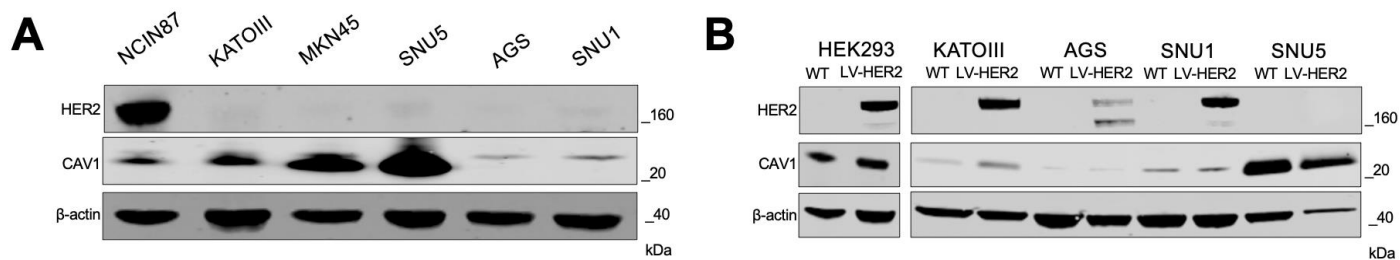
Supplementary Figure 3. CAV1 IHC in gastric tumor samples. CAV1-high: IHC 2+ and 3+ corresponds to cell clusters of moderate to strong membranous CAV1 staining. CAV1-low: IHC 1+ corresponds to cell clusters of weak to negative membranous CAV1 staining.



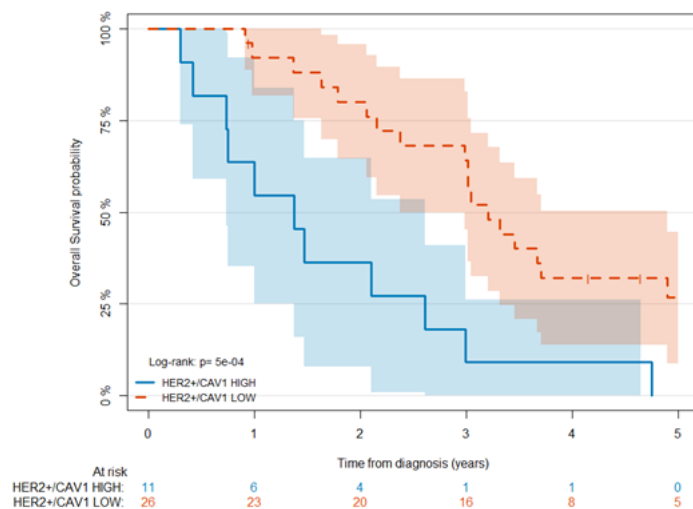
Supplementary Figure 4. Genomic alterations found in HER2⁺CAV1^{LOW} ($n = 20$) versus HER2⁺CAV1^{HIGH} ($n = 7$) gastric tumor tissues. (**Left Panel**) The rectangles with blue color highlight the absence of *PIK3CA* mutations in CAV1-high tumors. The rectangles with purple color highlight the absence of *PTEN* alterations in CAV1-low tumors. (**Right Panel**) The rectangles with yellow color highlight the presence of *MET* and *EGFR* amplification in CAV1-low tumors.



Supplementary Figure 5. Hematoxylin & Eosin (H&E), confocal images, and quantification of immunofluorescence staining of HER2 (green color) and CAV1 (red color) in human HER2-expressing gastric tumors. In blue color is cell nuclei. Tumors were classified as CAV1-high (Patient #1, #35, and #2) and CAV1-low (Patients #3, #5, #4, and #14). HER2 IF shows a predominant presence at the cell membrane in CAV1-low tumors. The graphs plot protein intensity per unit area, calculated by quantifying IF images (mean \pm S.E.M, n = 3).

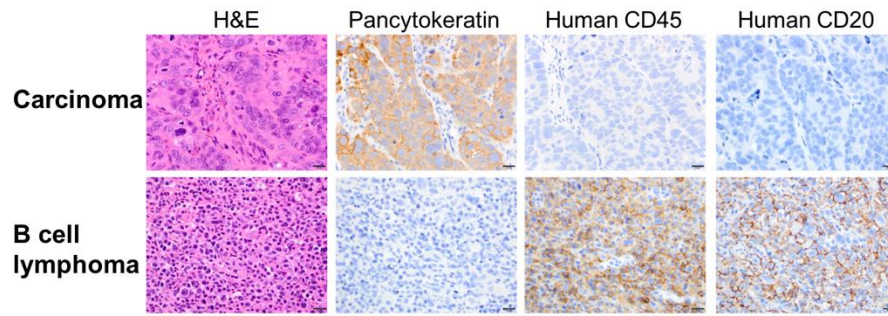


Supplementary Figure 6. (A) Western blot of HER2 and CAV1 in the total lysates of NCIN87, KATOIII, MKN45, SNU5, AGS, and SNU1 gastric cancer cells. (B) Western blot of HER2 and CAV1 in KATOIII, AGS, SNU1, and SNU5 gastric cancer cell lines wild-type (WT) and sublines stably expressing HER2 (LV-HER2). HEK293 WT and HEK293 LV-HER2 are also shown as controls. The protocols herein used did not allow for the successful generation of LV-HER2 in MKN45 and SNU5 cell lines containing the highest CAV1 expression.

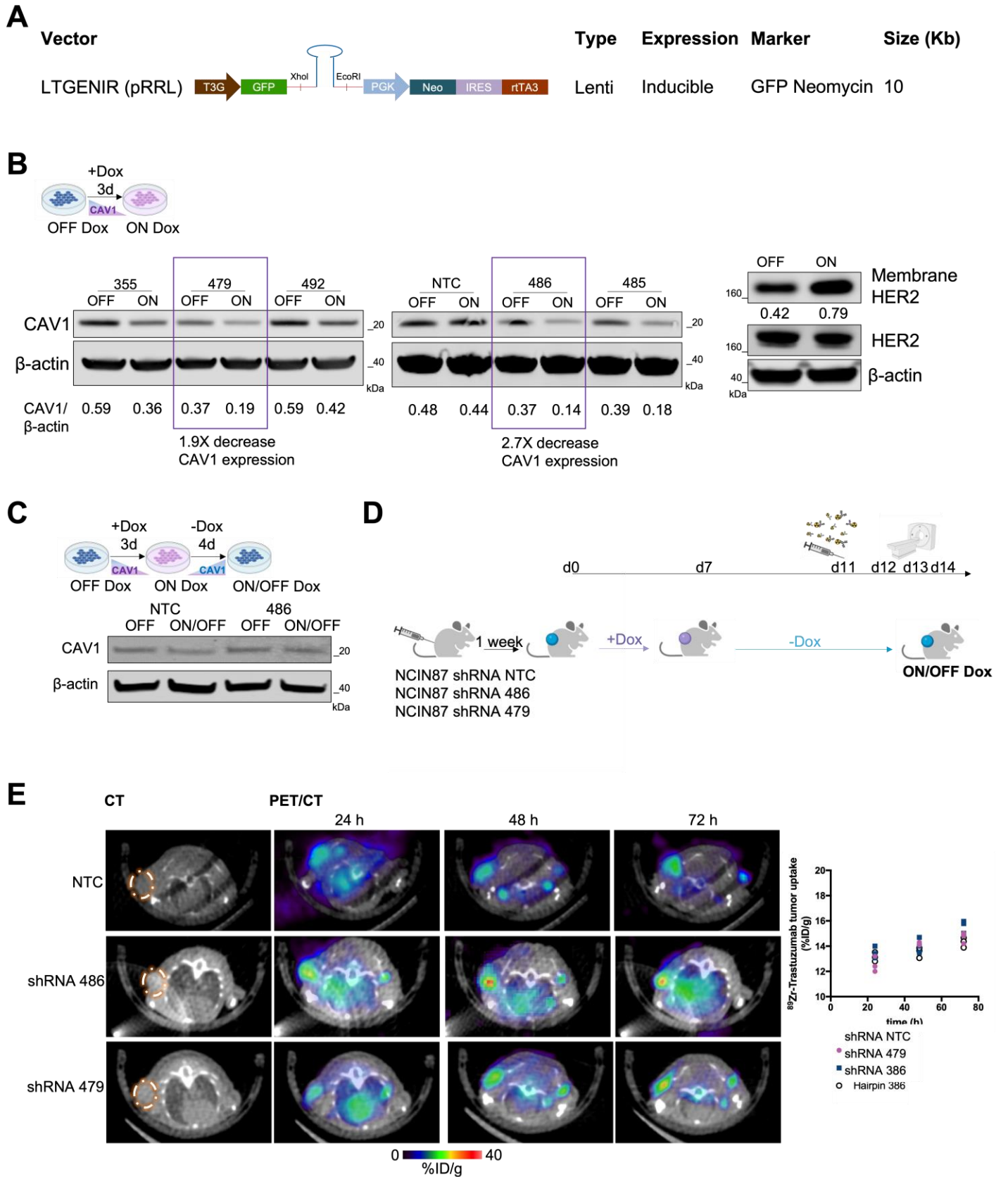


Characteristic	At 2 years	At 5 years
Group		
HER2 ⁺ /CAV1 ^{HIGH}	36% (8%, 65%)	0%
HER2 ⁺ /CAV1 ^{LOW}	80% (65%, 96%)	27% (9%, 45%)

Supplementary Figure 7. Kaplan-Meier analyses of CAV1 expression and GC disease outcome in patients treated with Trastuzumab that did not receive chemotherapy ($n = 37$ patients). Patients with HER2⁺/CAV1^{HIGH} (blue color, $n = 11$ patients) phenotype have a worse survival than HER2⁺/CAV1^{LOW} (red, $n = 26$ patients). Log rank; $p < 5 \times 10^{-4}$.

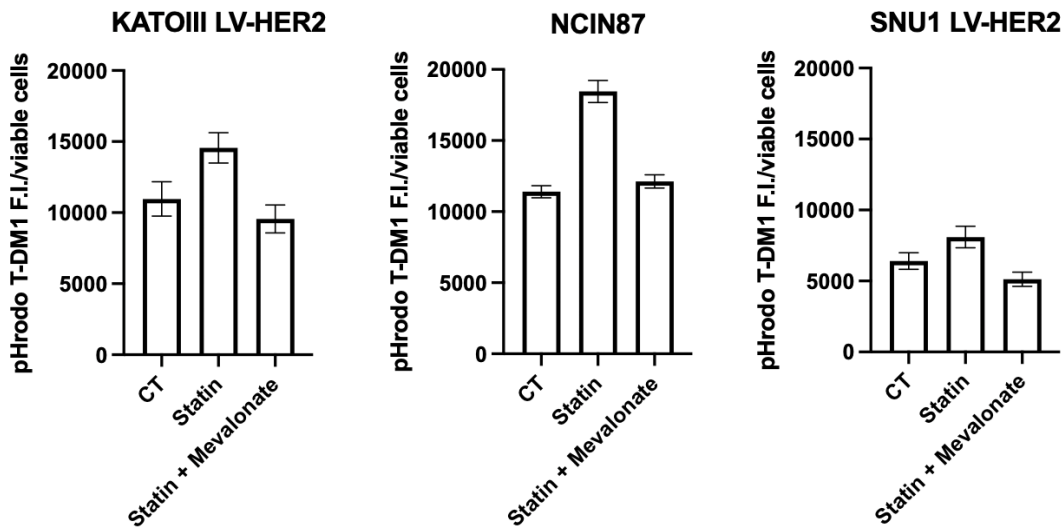


Supplementary Figure 8. Hematoxylin & Eosin (H&E) and immunohistochemical detection of pancytokeratin, human CD45, and human CD20 in PDX samples. Carcinomas were confirmed by IHC pancytokeratin⁺/CD45⁻/CD20⁻. B cell lymphomas excluded from the studies were IHC pancytokeratin⁻/CD45⁺/CD20⁺. Scale bar, 20 μ m.

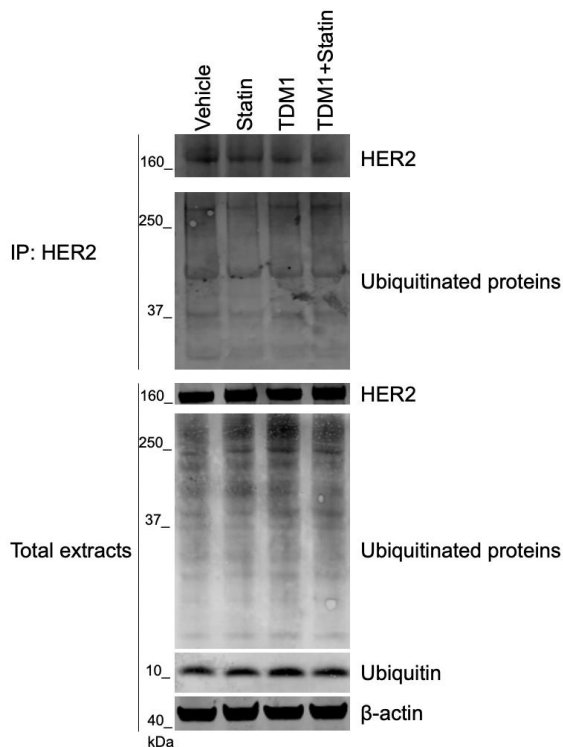


Supplementary Figure 9. (A) LT3GENIR4(pRRL) vector used to generate the tetracycline-inducible shRNA CAV1 Tet-On system. This backbone contains a neomycin selection and an inducible Dox system (Tet-On) that allows for the depletion of CAV1 in the presence of Dox. (B) Western blot of CAV1 and HER2 (membrane and total protein levels) in NCIN87 Tet-On systems using 5 different shRNA against CAV1 and 1 control NTC shRNA. Western blots show CAV1 depletion in cells incubated with 1 μ g/mL Dox for 3 days.

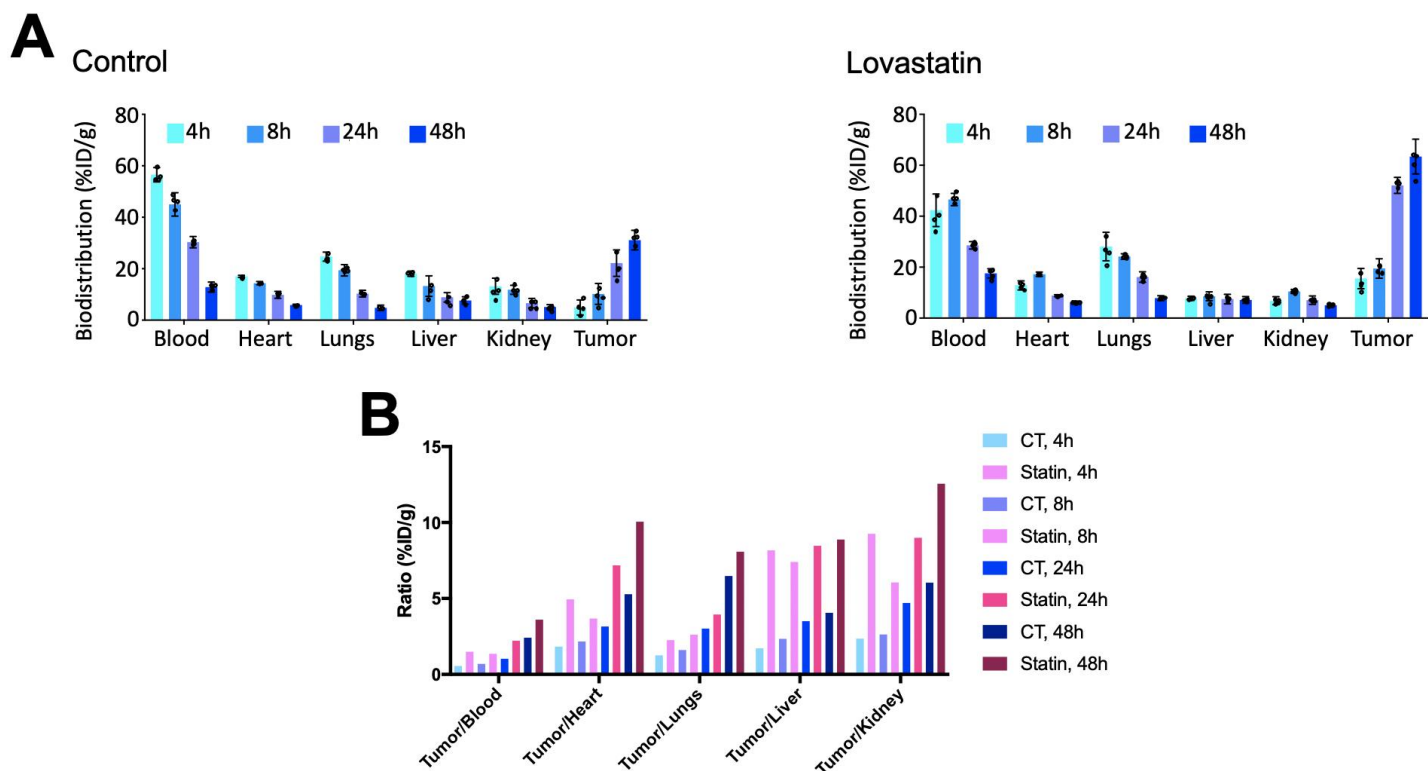
Dox treatment induced higher CAV1 depletion in 479 shRNA and 486 shRNA compared with 355, 492, 485 and were, therefore, used in subsequent assays. **(C)** Western blot of CAV1 in the NCIN87 Tet-On system using the shRNA 486 in the absence of Dox (OFF) or in cells treated with 1 $\mu\text{g}/\text{mL}$ Dox for 3 days and then incubated with media in the absence of Dox for 4 days (ON/OFF). The ON/OFF Dox schedule allows for temporal modulation of CAV1 protein levels. **(D)** Schematic of preclinical PET imaging studies using the NCIN87 Tet-On system and an ON/OFF Dox treatment. Athymic nude mice bearing s.c. NCIN87 shRNA NTC, shRNA 486, or shRNA 479 xenografts were orally administered with 10 mg/mL of Dox for 7 days. Mice were then orally administered PBS for 4 days. On day 11, mice were intravenously administered with [^{89}Zr]Zr-DFO-TDM1 (6.66–7.4 Mbq, 45–50 μg protein) and PET images recorded at 24, 48, and 72 h p.i. [^{89}Zr]Zr-DFO-TDM1. **(E)** Representative transversal PET images at 24, 48, and 72 h p.i. [^{89}Zr]Zr-DFO-TDM1 in athymic nude mice bearing s.c. NCIN87 Tet-On xenografts and ON/OFF Dox. Xenografts were obtained using NCIN87 shRNA NTC, shRNA 479, and shRNA 386 cell lines. Dox treatment and ^{89}Zr -labeled TDM1 injection were performed as described in panel **D**. The graph plots percentage of injected dose per gram (%ID/g) of TDM1 in tumors, calculated by quantifying regions of interest (ROIs) in the PET images.



Supplementary Figure 10. TDM1 internalization in NCIN87 GC cells wild-type (WT), KATOIII and SNU1 GC sublines stably expressing HER2 (LV-HER2) in the presence and absence of lovastatin and mevalonate (n = 10).

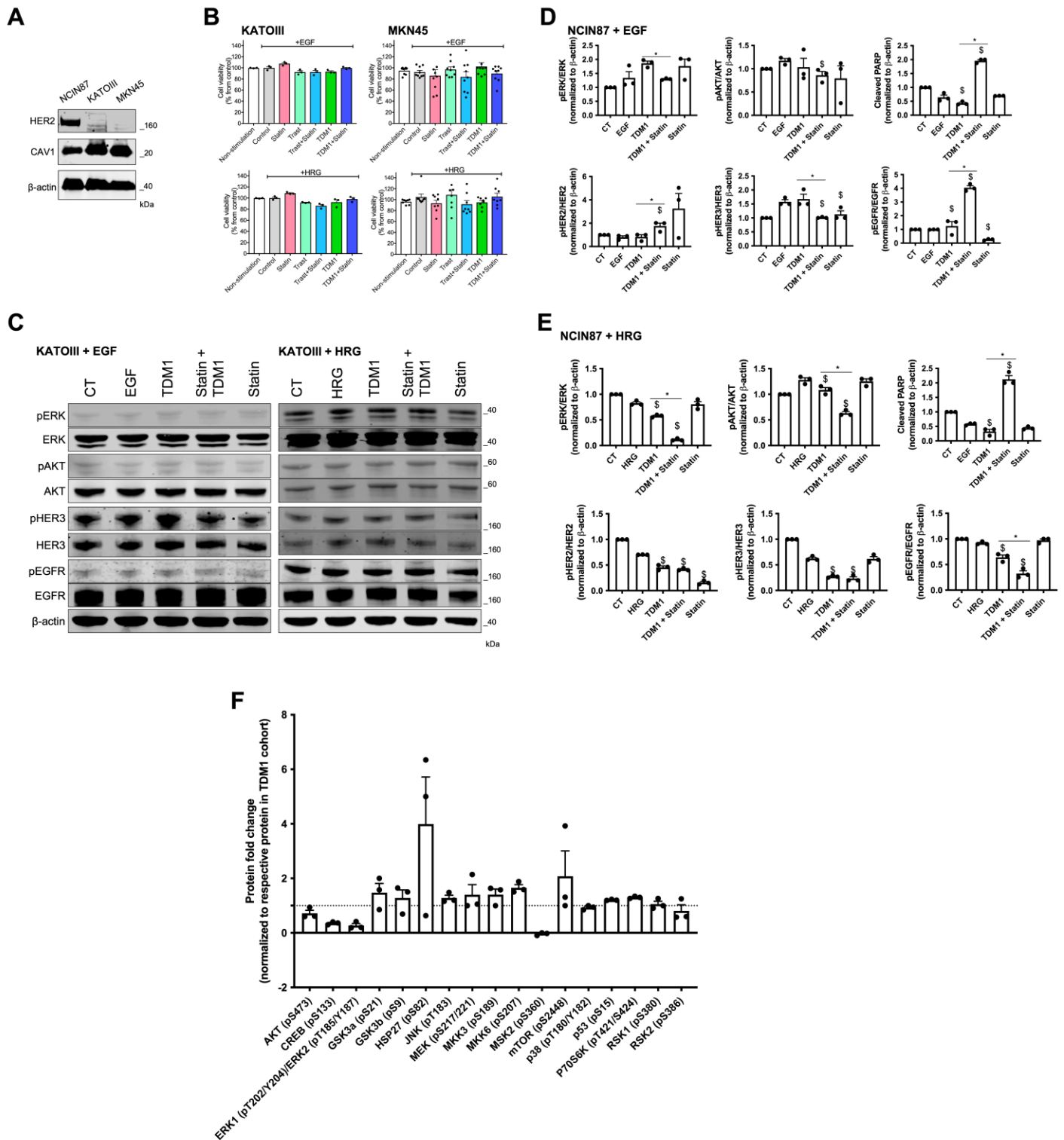


Supplementary Figure 11. Western blots are shown for HER2, ubiquitinated proteins, and ubiquitin from total NCIN87 cells extracts or extracts obtained after immunoprecipitation (IP) with anti-HER2 antibodies. Cells were incubated with TDM1 10 μ g/mL of TDM1 or vehicle as control, together with lovastatin in the presence of the proteasome inhibitor MG-132 (10 μ M) for 4 h at 37°C. β -actin was used as the loading control.



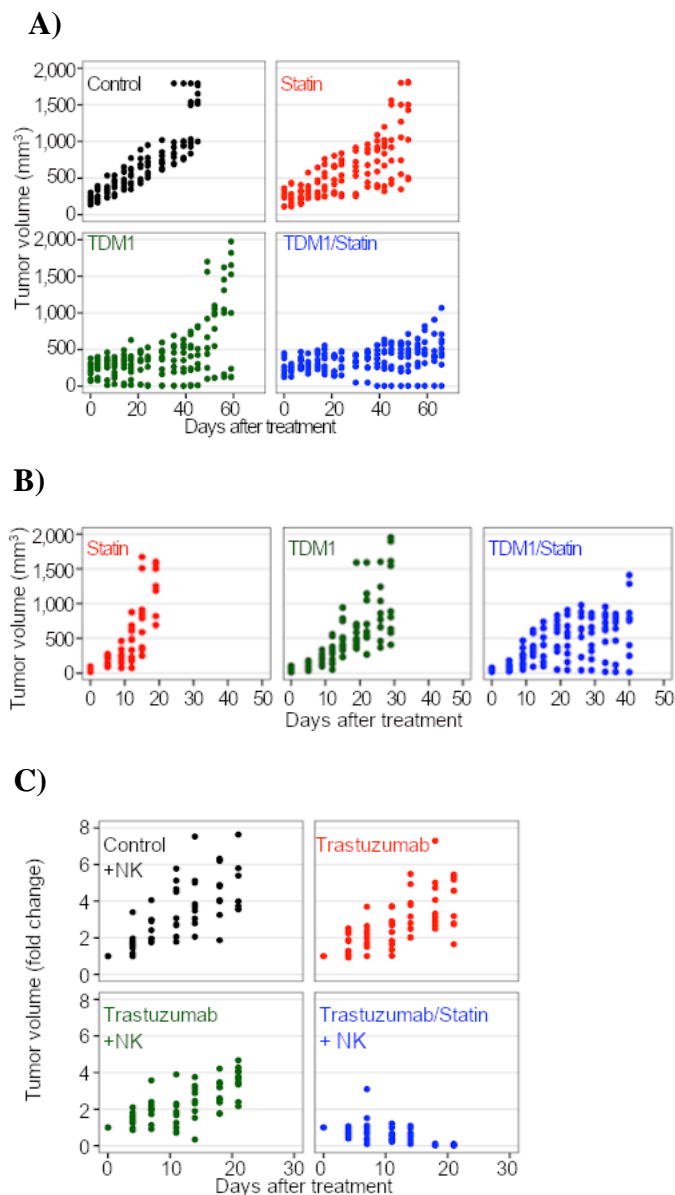
Supplementary Figure 12. Biodistribution data (A) and tumor-to-organs ratio (B) at 4, 8, 24, and 48 h p.i. of [^{89}Zr]Zr-DFO-TDM1 in athymic nude mice bearing s.c. NCIN87 gastric tumors. Lovastatin (8.3 mg/kg of mice) was orally administered 12 h prior and at the

same time as the tail vein injection of [⁸⁹Zr]Zr-DFO-TDM1 (6.66–7.4 Mbq, 45–50 μg protein). Bars, *n* = 4 mice per group, mean ± S.E.M. %ID/g, percentage of injected dose per gram.

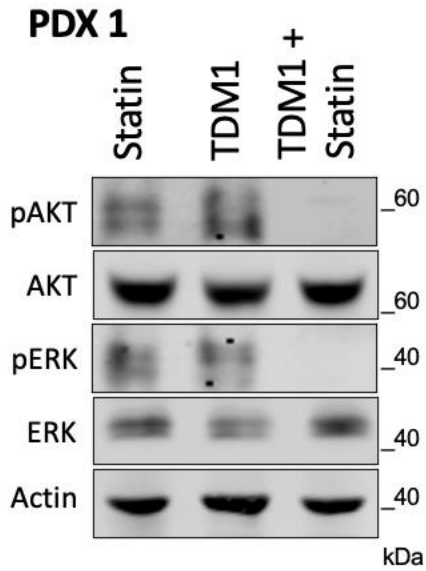


Supplementary Figure 13. (A) Western blot of HER2 and CAV1 in the total lysates of NCIN87, KATOIII, and MKN45 gastric cancer cells. (B) Cell viability of HER2-negative KATOIII and MKN45 gastric cancer cells at 48 h after cells incubation with trastuzumab and TDM1 alone or in combination with lovastatin. Cancer cells stimulated with 100 ng/mL EGF or HRG were incubated with 20 nM trastuzumab or TDM1. Lovastatin was added at a concentration of 25 μM. Non-stimulated cells were incubated in media in the absence

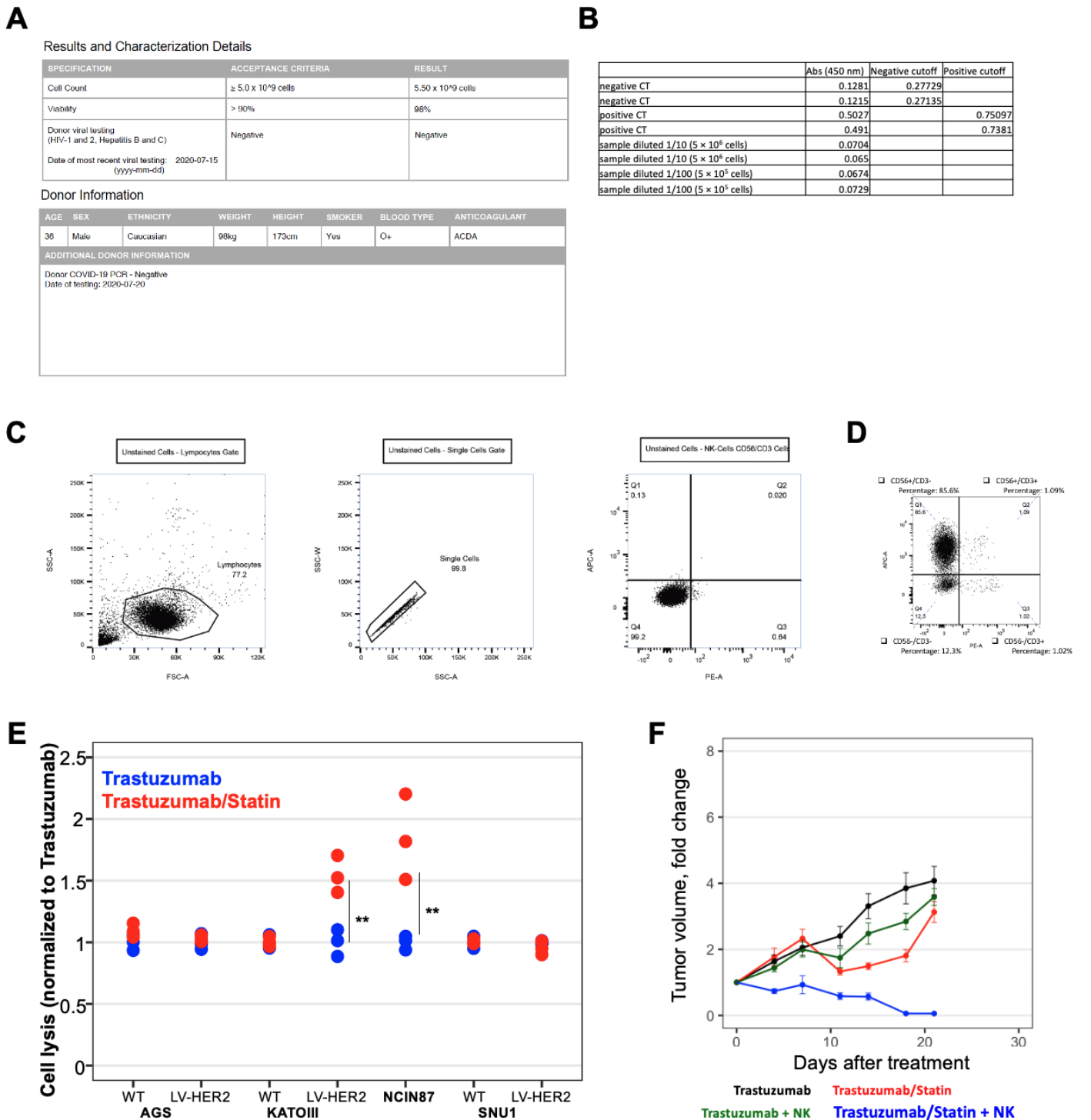
of antibody or growth factor-treated samples. Bars, $n = 3-4$ per group, mean \pm S.E.M. (C) Western blots of HER2-negative KATOIII GC cells at 48 h after cells incubation with TDM1 alone or in combination with lovastatin. (D,E) Quantification of western blots of HER2 signaling of HER2-expressing/CAV1^{HIGH} NCIN87 gastric cancer cells stimulated with EGF (D) or HRG (E) and treated with TDM1 alone or in combination lovastatin. Bars, $n = 3$ per group, mean \pm S.E.M. $^{\S}P < 0.05$ compared with control, $^*P < 0.05$ compared with TDM1 based on a Student's t -test. (F) MAPK signaling changes of TDM1/statin cohort (normalized to respective protein in TDM1 cohort) and determined using a MAPK phosphorylation antibody array.



Supplementary Figure 14. Superior *in vivo* therapeutic efficacy of TDM1 combined with lovastatin when compared with TDM1 alone in NCIN87 or PDX #1 xenografts (A,B). Lovastatin enhances Trastuzumab efficacy in NSG mice humanized with NK cells and bearing NCIN87 xenografts (C).

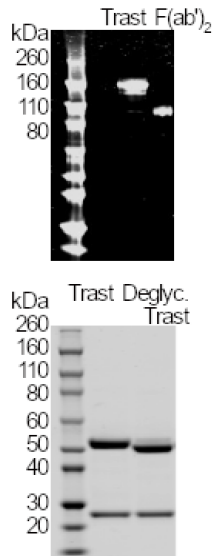


Supplementary Figure 15. Western blot analyses of AKT and ERK protein expression and phosphorylation in HER2⁺/CAV1^{HIGH} gastric PDX #1 at 35 days after treatment with lovastatin, TDM1, or TDM1/lovastatin. Intravenous TDM1 administration 5 mg/kg weekly (for 5 weeks) was started at day 0. Lovastatin (4.15 mg/kg of mice) was orally administered 12 h prior to and simultaneously with the intravenous injection of TDM1.

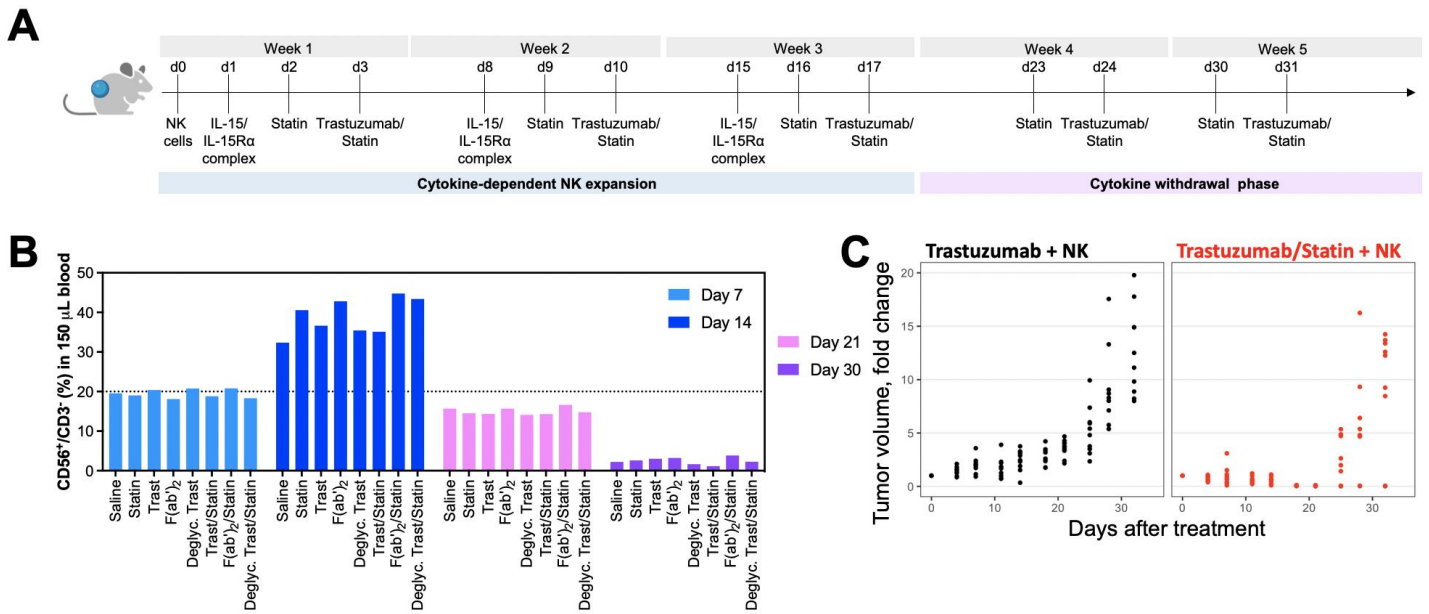


Supplementary Figure 16. (A) Information on the leukapheresis pack used for NK cell isolation. (B) ELISA test showing negative COVID-19 result on the day of NK cells isolation using a COVID-19 IgG ELISA Kit. The negative result for COVID-19 was further confirmed on the PCR result as shown in panel A. (C, D) Gating strategy used to identify NK cells by FACs. The EasySep Human NK Cell Enrichment Kit (negative selection) was used to separate NK cells from the leukapheresis pack. The isolated cells were fluorescently stained with APC CD56 and PE CD3, and analyzed by FACs. The NK cell population was confirmed by FACs as CD3⁺CD56⁺ cells. (E) Ability of trastuzumab or trastuzumab/lovastatin to mediate *in vitro* ADCC as determined with NK cells from a healthy donor. GC cells were incubated for 6 h with NK cells at a ratio of 50:1 (NK:GC cells) in the presence of 100 μ g/mL of trastuzumab in the absence or presence of lovastatin. Lovastatin enhances trastuzumab-mediated *in vitro* ADCC in HER2⁺ CAV1-expressing cells. Points, $n = 3$, ** $P < 0.01$ based on a Student's *t*-test. (F) Therapeutic studies of NSG mice and NSG mice humanized with freshly isolated NK cells.

NSG mice bearing subcutaneous HER2⁺/CAV1^{HIGH} NCIN87 xenografts were treated with lovastatin, trastuzumab, or a combination of trastuzumab/lovastatin ($n = 8-10$ mice per group, mean \pm S.E.M.). Intraperitoneal trastuzumab (5 mg/kg for 3 weeks) was started at day 0. Lovastatin (4.15 mg/kg of mice) was orally administered 12 h prior and at the same time as the injection of trastuzumab.

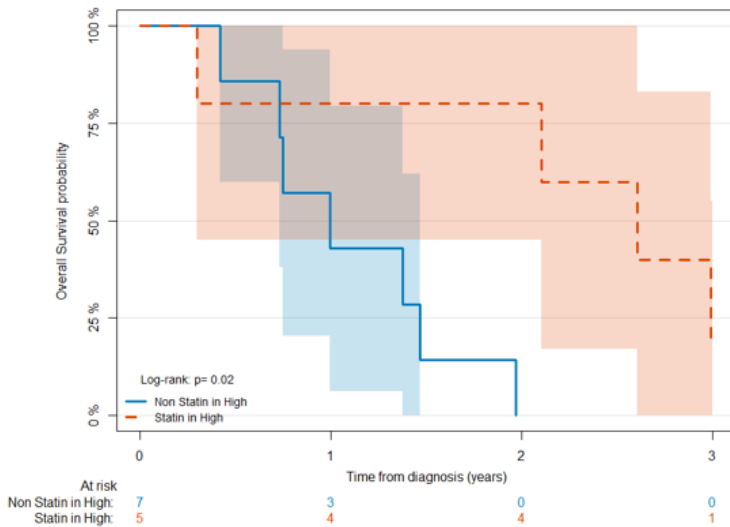


Supplementary Figure 17. SDS-PAGE of Trastuzumab F(ab')₂ fragments (top panel) or deglycosylated Trastuzumab (bottom panel). Trast, Trastuzumab. Deglyc, Deglycosylated.



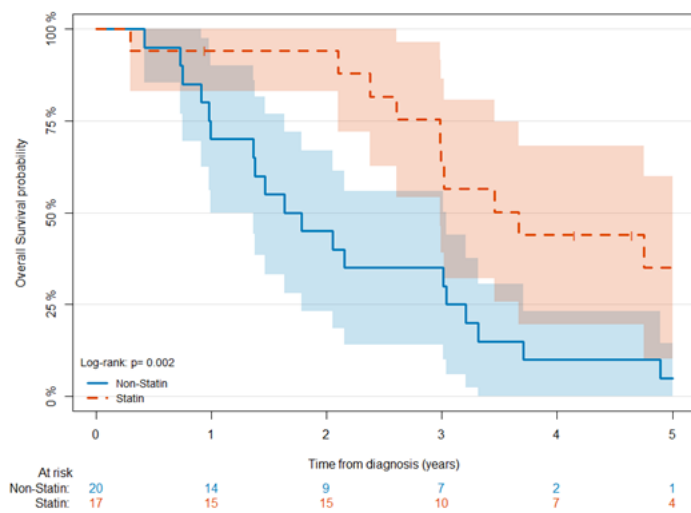
Supplementary Figure 18. (A) NSG mice bearing NCIN87 xenografts were intravenously injected with 1×10^6 human NK cells at day 0. One day after NK cells tail vein injection, the IL-15/IL-15R α complex was intraperitoneally administered at a dose of 1.25 μ g/mouse. Trastuzumab or trastuzumab/lovastatin efficacy was then evaluated during a cytokine-dependent NK expansion phase (week 1 to week 3) and a cytokine withdrawal phase (week 4 to week 5). (B) Percentage of human NK cells in 150 μ L of murine blood collected at day 7, day 14, day 21, and day 30 after intravenous injection of NK cells. Bars, $n = 2$ mice per group, mean \pm S.E.M. (C) Tumor volumes (fold change) as a function of time in trastuzumab or trastuzumab/lovastatin in individual NSG mice humanized with NK cells and bearing NCIN87 xenografts ($n = 10$ mice per group). In the trastuzumab/lovastatin cohort, 3/10 mice showed remnant tumors during the NK phase expansion (week 1–3) and cytokine withdrawal phase (week 4–5). On the other hand, 7/10 mice in the

trastuzumab/lovastatin cohort demonstrated similarly sized tumors compared with the trastuzumab cohort during the cytokine withdrawal phase.



Characteristic	At 2 years	At 3 years
Group		
Non-Statins in CAV1-high	0%	0%
Statins in CAV1-high	80% (45%, 100%)	20% (0%, 55%)

Supplementary Figure 19. Kaplan-Meier analysis of statin use and HER2-expressing CAV1-high GC disease outcome in patients treated with trastuzumab. CAV1-high HER2⁺ GC without statin treatment (blue color, $n = 7$) have a worse survival than patients treated with statin (red color, $n = 5$). *Log rank; $p=0.02$.*



Characteristic	At 2 years	At 5 years
Group		
Non-Statin	45% (23%, 67%)	5% (0%, 15%)
Statin	94% (83%, 100%)	35% (10%, 60%)

Supplementary Figure 20. Kaplan-Meier analysis of statin use and HER2-expressing GC disease outcome in patients treated with trastuzumab that did not chemotherapy regimens. Non-statin users (blue color, $n = 7$) have a worse survival than patients treated with statin (red color, $n = 5$). *Log rank; $p=0.002$.*